Exploring the Bandwidth Limits of ZTE Imaging

Markus Weiger[1], David Otto Brunner[1], Martin Tabbert[2], Matteo Pavan[1], Thomas Schmid[1], and Klaas Paul Pruessmann[1]
[1]*Institute for Biomedical Engineering, University and ETH Zurich, Zurich, Switzerland,* [2]*Bruker BioSpin MRI GmbH, Ettlingen, Germany*

Introduction MRI of samples with short transverse relaxation times can be very efficiently performed with zero echo time (ZTE) imaging [1-5]. In this 3D radial technique, centre-out encoding at immediate full speed is achieved by setting the readout gradient before excitation with a short hard-pulse. Data obtained in this way are incomplete in the *k*-space centre due to the initial dead time Δ of the RF chain (Fig. 1a). This *k*-space gap can be addressed by radial acquisition oversampling *ov* and algebraic reconstruction (AR), involving finite support extrapolation [6, 7]. The ZTE approach has been successfully used for imaging samples with T2s of several hundreds of µs, using acquisition bandwidths *bw* of 100-200 kHz [8, 9]. Targeting even shorter T2, however, requires larger bandwidth and hence shorter dwell time *dw*, increasing the relative gap size Δ counted in units of *dw*. The behaviour of noise with increasing Δ emerged to be rather benign, related to high statistical power in the centre of the 3D radial scheme [10]. However, at large Δ, ZTE images have still been observed to exhibit low-frequency artefacts (Fig. 1b) that must be attributed to non-random signal components but could not otherwise be explained so far. To elucidate this issue and eventually boost feasible ZTE bandwidths, in this work the spatial response of ZTE imaging as a function of Δ is investigated and the practical bandwidth limits are explored by simulations and phantom experiments.

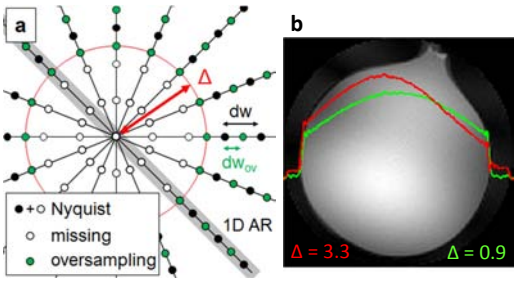

Figure 1 a) ZTE sampling scheme with dwell time *dw*, oversampling *ov*, and gap Δ. b) ZTE image acquired with Δ = 3.3 *dw*, exhibiting low-frequency artefacts. Reference profile with Δ = 0.9 *dw* shows only B1 non-uniformity.

Theory In ZTE image reconstruction, 1D projections are first obtained by AR from pairs of opposite readouts, which are then combined by standard 3D gridding. The specific AR part employs the reconstruction matrix **F** which is obtained by matrix inversion to fulfil the spatial response condition **FE** = **Id** where the encoding matrix **E** is given on the image voxel grid. Hence a voxel's spatial response function (SRF) quantifying the contributions of all locations in space is required to be 1 in the centre of the target voxel and 0 in all other voxel centres. In addition, finite support is implied by limiting **E** to the desired field-of-view (FOV), thus allowing arbitrary SRF behaviour outside. Continuous SRFs are calculated according to **SRF** = **FE'** where the rows of **E'** are continuous representations of the encoding functions in the range of interest [11].

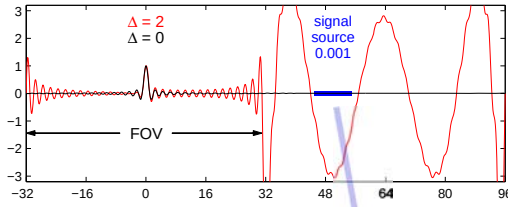

Figure 2 Spatial response function (SRF) for Δ = 0 and 2 calculated in- and outside the FOV of 64 pixels with *ov* = 2.

Experimental Using a 9.4 T Bruker animal MRI system, phantom experiments were performed with 19F to minimise background signal (see below) [12]. With the same rationale, a dedicated T/R saddle volume RF coil was built, using a PMMA base and Teflon-free trimmer capacitors. As a long-T2 phantom a glass sphere of ∅ = 50 mm was filled with doped Hexafluorobenzene of T2 ≈ 120 ms. As a short-T2 phantom a cylindrical Teflon disc with ∅ = 52 mm and T2 ≈ 25 µs was used. All experiments were performed with *ov* = 4, full Nyquist angular encoding, RF pulse duration = 2 µs, and flip angle = 2.7°. Further parameters for the sphere | Teflon disc were FOV = 60 | 80 mm, matrix = 128 | 64, *bw* = 100 | 100-500 kHz, averages = 16 | 4, TR = 2 | 1 ms, and Δ = 1.0-4.0 | 1.0-3.8 dw.

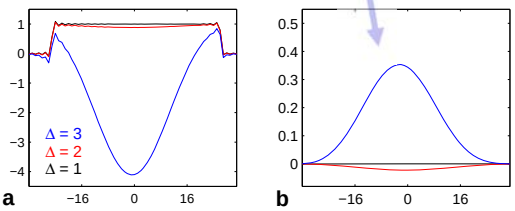

Figure 3 Simulated 1D images with SRF-related artefacts originating from a) inside and b) outside the FOV.

Results 1D SRFs were calculated for a range extending beyond the FOV (Fig. 2). For Δ = 0, the typical Sinc shape is obtained. For Δ = 2, the SRF develops considerably enhanced side-lobes in the FOV while still fulfilling the spatial response condition. The effect of these SRF changes is demonstrated with simulated 1D images of a box-shaped object of unit amplitude (Fig. 3a). For Δ = 1, the result is only affected by common Gibbs ringing. For Δ = 2, minor low-frequency artefacts occur while for Δ = 3 the 1D image is heavily distorted. In addition, Fig. 2 also shows that *outside* the FOV even larger SRF amplitudes occur. The associated effect on the 1D image was studied by assuming a hypothetical low-amplitude signal source in this "forbidden" range (see Fig. 2), demonstrating that the signal appears with strong amplification as a low-frequency artefact in the image (Fig. 3b). On this basis, both SRF imperfections and external signal sources might explain the problems observed in Fig. 1b. However, in contrast to the 1D behaviour, simulated 3D ZTE images (Fig. 4a) show that despite the strong distortions in the projections (cf. Fig. 3a), actually artefact-free images are still obtained for the initially critical Δ = 3.3 (cf. Fig. 1b). This benign behaviour is due to destructive interference of incoherent artefacts for different projections in the highly oversampled *k*-space centre, as similarly observed for noise [10]. With this insight, measurements were performed with the previously mentioned 19F setup to minimise background signal from outside the FOV (cf. Fig. 3b). As predicted, the sphere data in Fig. 4b show that in this way, artefacts could be greatly reduced compared with Fig. 1b. These short-T2 capabilities were directly employed for ZTE imaging of Teflon at unprecedented high bandwidth of 500 kHz, using Δ = 3.8 (Fig. 5).

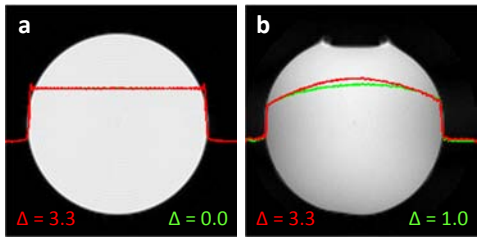

Figure 4 a) Simulated and b) measured 3D images with Δ = 3.3. Residual artefacts in b) stem from background signal.

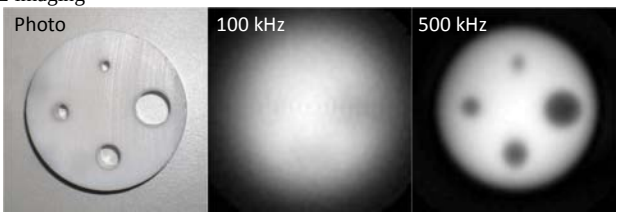

Figure 5 Fluorine 3D ZTE imaging of a Teflon cylinder with T2 ≈ 25 µs, using Δ = 3.8, matrix size = 64, and scan time = 53 s.

Discussion Large *k*-space gaps in ZTE imaging affect the SRF both inside and outside the FOV, leading to low-frequency artefacts in 1D reconstructions. Nevertheless, artefact-free final 3D images can be obtained with remarkably large gaps due to averaging in central *k*-space inherent to radial acquisition. It is essential, however, to strictly avoid SRF-related artefacts due to amplification of any signal sources outside the FOV, e.g. from the RF coil. It has been demonstrated that in doing so, Δ > 3 and bandwidths up to 500 kHz can be realised. Targeting even larger Δ will require further reduction of background signal, which is particularly demanding for 1H imaging [12]. Furthermore, the increasing SRF effects from inside the FOV might be addressed by spatial response optimisation [13]. In this way, ZTE imaging can approach T2s even below 100 µs without compromising on spatial resolution as inherent to most related techniques. Thus, new tissues and materials may become accessible with MRI. The remaining challenges along this path concern signal-to-noise, RF pulse bandwidth, and specific absorption rate.

References **[1]** Hafner S, MRI 12 (1994) 1047. **[2]** Madio DP, MRM 34 (1995) 525. **[3]** Kuethe DO, MRM 39 (1998) 85. **[4]** Wu Y, Calcif Tissue Int 62 (1998) 512. **[5]** Weiger M, EMR DOI: 10.1002/9780470034590.emrstm1292. **[6]** Jackson J, MRM 11 (1989) 248. **[7]** Kuethe DO, JMR 139 (1999) 18. **[8]** Kuethe DO, MRM 57 (2007) 1058. **[9]** Weiger M, NMR Biomed 25 (2012) 1144. **[10]** Weiger M, ISMRM 2011, 747. **[11]** Pruessmann KP, NMR Biomed 19 (2006) 288. **[12]** Horch RA, MRM 64 (2010) 1652. **[13]** Tsao J, ISMRM 2003, 14.